Green Chemistry

PAPER

View Article Online
View Journal | View Issue

Cite this: *Green Chem.*, 2024, **26**, 11673

Postliminary treatment of food-waste digestate *via* combined hydrothermal carbonization and microbial fuel cell for bio-energy recovery: a comparative life cycle impact assessment†

Shraddha Yadav,[a] Manikanta M. Doki,[b] Makarand M. Ghangrekar *[a,b,c] and Brajesh K. Dubey[b]

Anaerobic digestion (AD) is the predominant technique for transforming food-waste into biomethane, yet the dewatering and valorisation of the resultant digestate present a significant downstream technical challenge. This investigation provides an advanced digestate management approach for resource recovery through the synergistic integration of hydrothermal carbonization (HTC) with anaerobic digestion. The integrated system resulted in biomethane (~466 mL g^{-1} VS) and biocoal (hydrochar) with a high calorific value (~22 MJ kg^{-1}). The effect of HTC operating conditions including reaction temperature and time on the coalification degree has been investigated. Additionally, the by-product of HTC, *i.e.*, HTC process water was treated using the microbial fuel cell (MFC) with organic abatement efficiency of 76.0 ± 4.6% and power recovery of ~4.41 W m^{-3}. Further, the metagenomic analysis was conducted to affirm the high proliferation of specific electrogens (*Clostridia*) in the MFC. Distinctively, in this work, the impacts on the environment in eighteen different categories using life cycle assessment for the technologies AD, AD + HTC, and AD + HTC + MFC were also compared. The single score results demonstrated the least impact of the integrated AD + HTC + MFC on human health, ecosystem, and resource depletion. This highlights the potential of the integrated system for real-field applicability, sustainable digestate management, and bioenergy recovery.

Received 15th August 2024,
Accepted 14th October 2024

DOI: 10.1039/d4gc04081c

rsc.li/greenchem

Introduction

Present research and commercial endeavours focus on extracting resources from waste streams, driven by the potential to enhance both the economic and environmental efficiency of the waste-treatment process.[1,2] Identifying opportunities for resource recovery can transform a treatment initiative into a profitable venture with forecasted economic gains. Additionally, the distinct proposition of resource recovery can support the paradigm shift from linear economy to circular economy and sustainable development goals of the world.[3] In the realm of food, food industry, marketplaces, and residential places, resource recovery has been a subject of exploration for several decades.[4] This exploration encompasses the separation of valuable materials from industrial food waste (FW) and the utilization of FW as a substrate or reactant in the production of valuable compounds through fermentation or traditional chemical processes.[5]

Biomethane produced *via* an anaerobic digestion (AD) process from renewable waste biomass, such as FW, represents a promising biofuel with ideal properties to replace fossil-based petroleum products.[6–9] Plant-based biomass absorbs carbon during its growth, and biofuel generated from it releases carbon emissions on combustion, which returns to the atmosphere. Hence, ensuring the modern second-generation biofuel as a near Net Zero-Emissions biofuels.[10] In the Net Zero Emissions Scenario, biofuel production is projected to surpass ten exajoules by 2030, necessitating an annual growth rate of approximately 11%.[11] The expansion of advanced feedstock utilization is also imperative. Biofuels derived from waste, residues, and non-food energy crops are anticipated to contribute more than 40% to the overall biofuel demand by 2030, a substantial increase from the 9% share observed in 2021.[12]

Despite the success of AD plants at the field or industrial scales, managing anaerobic digestate remains a challenge. It is

[a]*School of Environmental Science and Engineering, Indian Institute of Technology Kharagpur, Kharagpur, 721302 West Bengal, India.*
E-mail: ghangrekar@civil.iitkgp.ac.in
[b]*Department of Civil Engineering, Indian Institute of Technology Kharagpur, Kharagpur, 721302 West Bengal, India*
[c]*National Institute of Technology Puducherry, Karaikal, 609609, India*

† Electronic supplementary information (ESI) available. See DOI: https://doi.org/10.1039/d4gc04081c

estimated that 0.2–0.47 tons of FW digestate solids are generated for each ton of FW treated by AD.[13] Further, anaerobic digestate derived from FW (AD-FW) contains high concentrations of organics, proteins, carbohydrates, phosphate (PO_4^{3-}), ammonium (NH_4^+), potassium ion (K^+), nitrogen ion (N^+), and chloride ion (Cl^-). Therefore, repurposing the AD-FW into renewable and value-added products like biofertilizers, solid biofuels, and carbon-based materials demonstrates significant potential for various environmental applications.[14,15] For instance, a FW-to-energy facility based on AD in Hong Kong used to recycle source-separated FW into methane-rich biogas, which is used to generate energy, with a daily capacity of 200 tons.[16] The resultant AD-FW (around 20 tons per day) was composted and dewatered to be used in agriculture and landscaping. However, use as a biofertilizer or for pyrolysis would possess drawbacks such as ammonia volatilization, nitrate leaching, nutrient toxicity, dewatering cost, induced eutrophication, *etc*.[17] Hence, thermo-chemical treatment such as hydrothermal carbonization (HTC) emerged as an ideal approach for wet biomass valorisation, by eliminating energy-intensive precursor dewatering step.[16,18]

The HTC is a wet thermochemical process carried out at autogenous pressures (3.5–5.5 MPa) and temperatures ranging from 180 °C to 300 °C.[19,20] Further, HTC of digestate serves the advantages of enhanced dewaterability, hydrophobicity, high carbon sequestration, and generate solid biofuel, *i.e.*, hydrochar (HC).[21,22] According to previous studies, HC exhibited higher energy densification than raw digestate, better combustion characteristics, and calorific values in the range of 12–25 MJ kg^{-1} (dry basis), similar to that of lignite coal.[23] However, the secondary product generated during the HTC is the process water (termed as HTC-PW), which is rich in organics, furans, phenolic compounds, furfural, organic acids, ammonia, and other nutrients.[24,25] Treatment of this aqueous phase is necessary prior to disposal. For example, Kambo *et al.* reported the recirculation of HTC-PW in the HTC process and observed a significant increase in mass yield (5–10%) and energy yield (~15%) of HC.[26] In another investigation, Erdogan *et al.* utilized the HTC-PW for biogas production and obtained a volumetric methane content of 66.1%.[27] However, to the best of the author's knowledge, the valorisation of HTC-PW for the production of clean energy, *i.e.*, bio-electricity using microbial fuel cells (MFCs), is not unveiled yet. The MFC is a bioelectrochemical system that transforms chemical energy stored in an organic substrate into electrical energy in the presence of electro-active microorganisms.[28] Till now, the MFC technology has been adopted for domestic wastewater and different industrial wastewater including brewery wastewater, dairy wastewater, ethanol stillage, and mustard tuber wastewater.[29–32]

Therefore, the present investigation optimized the potential of AD-FW (from co-digestion of FW and up-flow anaerobic sludge blanket reactor (UASBR) sludge) derived HC as a solid fuel. The optimization was conducted in terms of high heating values (HHVs), fuel ratio (FR), functional, and combustion characteristics under different reaction time (2–6 h) and temperature (180–240 °C). Further, the novel valorisation of HTC-PW using MFC for bioelectricity generation under real environmental conditions has been performed and compared with synthetic wastewater. Additionally, the proliferation of the HTC-PW specific microbial genomes were analysed to support the outstanding power performance. This investigation is also the first of its kind, wherein the life cycle assessment (LCA) of the AD, AD + HTC, and AD + HTC + MFC system was performed for the comparative assessment of the integrated technology to treat 1 kg of FW and to analyse the environmental impacts.

Results and discussion

Resource 1: biomethane recovery from co-digested FW and UASBR sludge

The biochemical methane potential (BMP) analysis was conducted to determine the biogas and biomethane production for control and co-digestion (*i.e.*, FW + UASBR sludge) set-up. Under the optimal condition, *i.e.*, 37 °C for 60 days, the initial lag period was 8 days for co-digestion set-up, which was significantly less as compared to mono-digestion of FW (15 days). Here, the active UASBR sludge served both as inoculum and co-substrate with no lag period for biogas production. Later, biogas and biomethane production began to rise with the increase in experiment duration. Ultimately, the rate of biogas and biomethane production reached 726 ± 56 mL g^{-1} of volatile solids (VS) and 465.18 ± 20 mL g^{-1} of VS, from the digestion of FW + UASBR sludge, respectively (Fig. 1). This shows improved biodegradability and higher biogas production on adopting UASBR sludge as co-substrate with FW. The justification for the enhanced stability of the system in co-digestion processes is the co-substrates functioning as diluting agents for toxic chemicals such as ammonia or sodium ions.[33] Also, the present results correlate with the results obtained by Prabhu *et al.*, who investigated the co-digestion of FW and sewage sludge in the ratio of 1 : 2, yielding biogas of 823 mL g^{-1} of VS with methane content up to 60%.[34] In another investigation, Cabbai *et al.* reported the maximum biomethane production of 675 mL g^{-1} of VS on co-digestion of organic fraction of municipal solid waste with sewage sludge in 50 : 50 ratio by volume.[35] This showed the sufficient biodegradability of the substrate for biomethane recovery.

Resource 2: hydrochar (bio-coal) – physiochemical characterization

The AD-FW (by-product of AD) was transformed to HC using HTC technology. The physiochemical characteristics were evaluated, including proximate and ultimate analysis to determine the volatility and elemental composition of the precursor, *i.e.*, AD-FW and the as-synthesized HC. As depicted in Table 1, the HC yield (HCY) decreased with increasing hydrothermal temperature (from 180 °C to 240 °C) and retention time (2 h to 6 h), which might be due to hydrolysis, dehydration, decarboxylation, and decomposition of hemicellulose and lignocellulosic

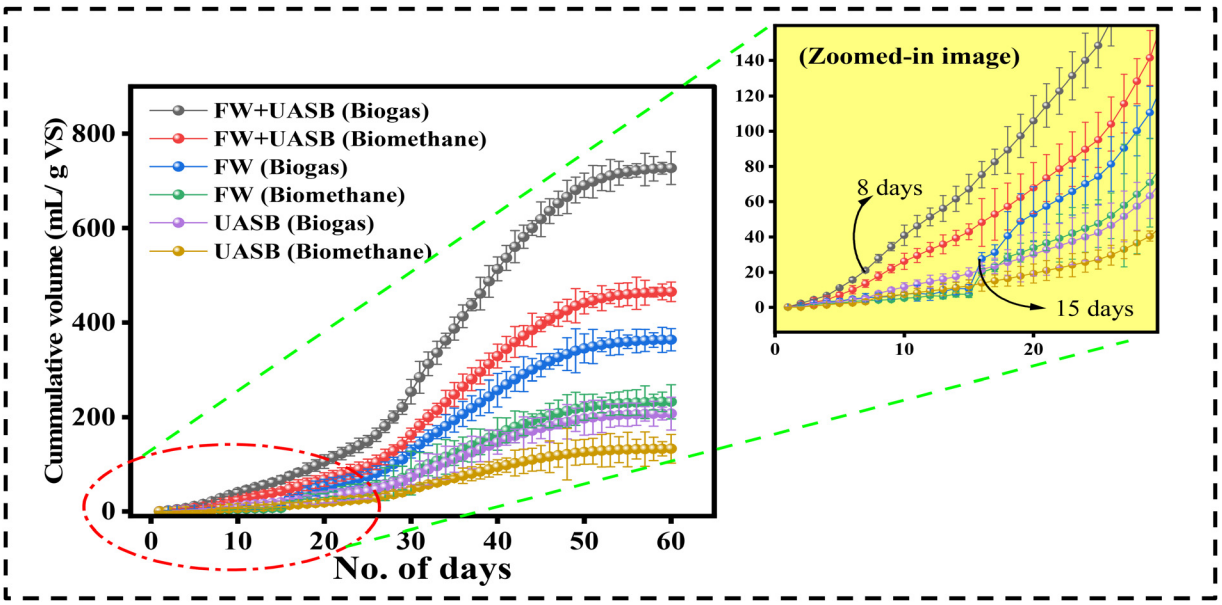

Fig. 1 Biogas and biomethane potential of co-digested FW and sludge from UASBR treating sewage (zoomed-in image: enlarged view for starting 20 days illustrating initial lag period).

Table 1 Proximate and ultimate analysis of precursor AD-FW and derived hydrochar at variable temperature and time

		HC (180 °C)			HC (210 °C)			HC (240 °C)		
Parameters	AD-FW	2 h	4 h	6 h	2 h	4 h	6 h	2 h	4 h	6 h
HCY (%)	—	60.2	56.8	55.2	57.6	54.5	51.2	50.8	48.2	47.3
VS (%)	70.5 ± 1.5	56.8 ± 0.8	51.2 ± 1.2	45.9 ± 0.5	45.7 ± 1.0	44.3 ± 1.1	42.6 ± 0.6	42 ± 1.3	40.6 ± 1.0	39.8 ± 1.0
FC (%)	16.7 ± 0.3	20.4 ± 0.5	21.9 ± 0.5	24.5 ± 1.1	20.9 ± 0.6	22.7 ± 1.0	24.6 ± 0.8	21.9 ± 0.2	23.5 ± 0.5	26.4 ± 1.5
Ash (%)	17.2 ± 1.2	17.5 ± 0.8	18.7 ± 0.3	18.9 ± 0.6	18.5 ± 1.1	19.2 ± 0.5	19.3 ± 0.6	19.1 ± 0.5	19.9 ± 1.0	20.4 ± 0.3
C (%)	42.30	43.90	45.67	51.20	45.20	54.76	54.0	48.90	53.10	56.20
H (%)	7.30	7.04	6.89	7.46	6.80	7.17	6.54	7.10	6.45	6.45
N (%)	4.13	3.45	3.14	2.06	2.35	1.37	1.2	1.88	1.88	1.56
S (%)	0.14	0.14	0.12	0.11	0.10	0.12	0.12	0.12	0.12	0.10
O (%)	46.13	45.47	44.18	39.17	45.55	36.58	38.14	42	38.45	35.67
H/C	2.07	1.92	1.81	1.74	1.80	1.57	1.45	1.74	1.46	1.38
O/C	0.81	0.78	0.72	0.57	0.75	0.50	0.53	0.64	0.54	0.48
HHV	16.49	16.78	17.39	20.96	16.86	22.21	20.79	19.17	20.30	21.84

components in AD-FW.[36] At higher temperatures or elevated subcritical water conditions, the kinetics of water molecules intensify, facilitating the solubilization of complex organic constituents of biomass, consequently leading to a reduction in the production of HC.[37] Hence, the optimized reaction temperature and time, *i.e.*, 210 °C for 4 h, proved to be the most beneficial operating conditions to get better HCY. Consequently, the proximate analysis of HC revealed that the VS decreased, whereas the fixed carbon (FC) content enhanced with an increase in carbonization temperature.

The raw AD-FW exhibited 70.5 ± 1.5% of VS (based on dry wt.) and FC content of 16.7 ± 0.3%. The VS of HC was reduced to a minimum of 39.8 ± 1.0% (at 240 °C; 6 h), which can be ascribed to the higher volatilization of organics at the peak temperature and retention time during the carbonization process. The above results were similar to the findings of Gao *et al.* who reported a maximum of 29.9% FC for HC synthesized at a peak temperature of 240 °C and retention time of 10 h.[38] On the other hand, the FC content reached a maximum of 26.4 ± 1.5% (at 240 °C; 6 h), which was caused by increased organic structure repolymerization and aromatization that turned into more stable and condensed carbon-rich structures.

As FC is the carbon content that doesn't volatilize during combustion, hence higher FC showcases a biofuel with high energy content, better stability during combustion, less pollution, and better control of the carbon process.[37,39] The increase in ash content during the HTC can be attributed to the disintegration of volatile components from the biomass into the HTC-PW fraction and the precipitation of salts present in the biomass onto the HC as the reaction mixture cools down. Both of these processes result in the incorporation

of inorganic substances into the HC, leading to an increase in ash content.[40] Results of the elemental analysis revealed a positive correlation between the C% and HTC temperature under constant retention time. The C% of raw AD-FW was 42.30%, which enhanced to 43.90%, 45.20%, and 48.90% for 180 °C (2 h), 210 °C (2 h), and 240 °C (2 h) respectively.

However, by extending the HTC retention time from 2 h to 6 h, the C% reached a maximum of 56.20%, which is attributed to the extensive carbonization, removal of VS, aromatization, and condensation reactions, thus overall contributing to the C enrichment in HC. Further, in contradiction, the H%, O%, and N% showed a decremental trend in comparison to raw feedstock. The decrement in H% and O% might be due to dehydration, decarboxylation, and deoxygenation reactions taking place during the HTC process. Furthermore, a decrease in N% with increased retention time and HTC severity contributed to the solubilization of the proteinaceous substances in the aqueous phase (*i.e.*, HTC-PW) of the HTC and enhanced deamination of AD-FW.[41,42] Additionally, factors like the removal of volatile nitrogen compounds, conversion to gases like ammonia, and decomposition of complex organic nitrogen compounds under thermal treatment would also be responsible for decreased N% in HC.[42]

Fuel characteristics of AD-FW hydrochar and comparative assessment with respect to coal of different ranks. The intensity of coalification was evaluated based on H/C and O/C atomic ratio as depicted in the Van Krevelen diagram (Fig. 2a and b). The diagram demonstrates a comparative assessment based on the coalification degree and fuel characteristics of the synthesized HC and other fossil fuels, such as anthracite, coal, lignite, peat, and biomass. Conventionally, a lower H/C and O/C ratio signifies a higher magnitude of coalification and better energy potential of the as-synthesized HC.[43] In the present investigation, the H/C and O/C ratio of raw AD-FW, HC at the lowest temperature–time combination (180 °C, 2 h), and the HC at highest temperature–time combination (240 °C, 6 h) were 2.07, 0.81 (maximum); 1.92, 0.78; and 1.38, 0.48 (minimum), respectively. A declining trend in H/C and O/C ratio with an upsurge in HTC temperature and time was predominately due to the dehydration, decarboxylation, and demethanation reactions occurring during the HTC process. Thereby, resulting in the release of CO_2 and H_2O.[43]

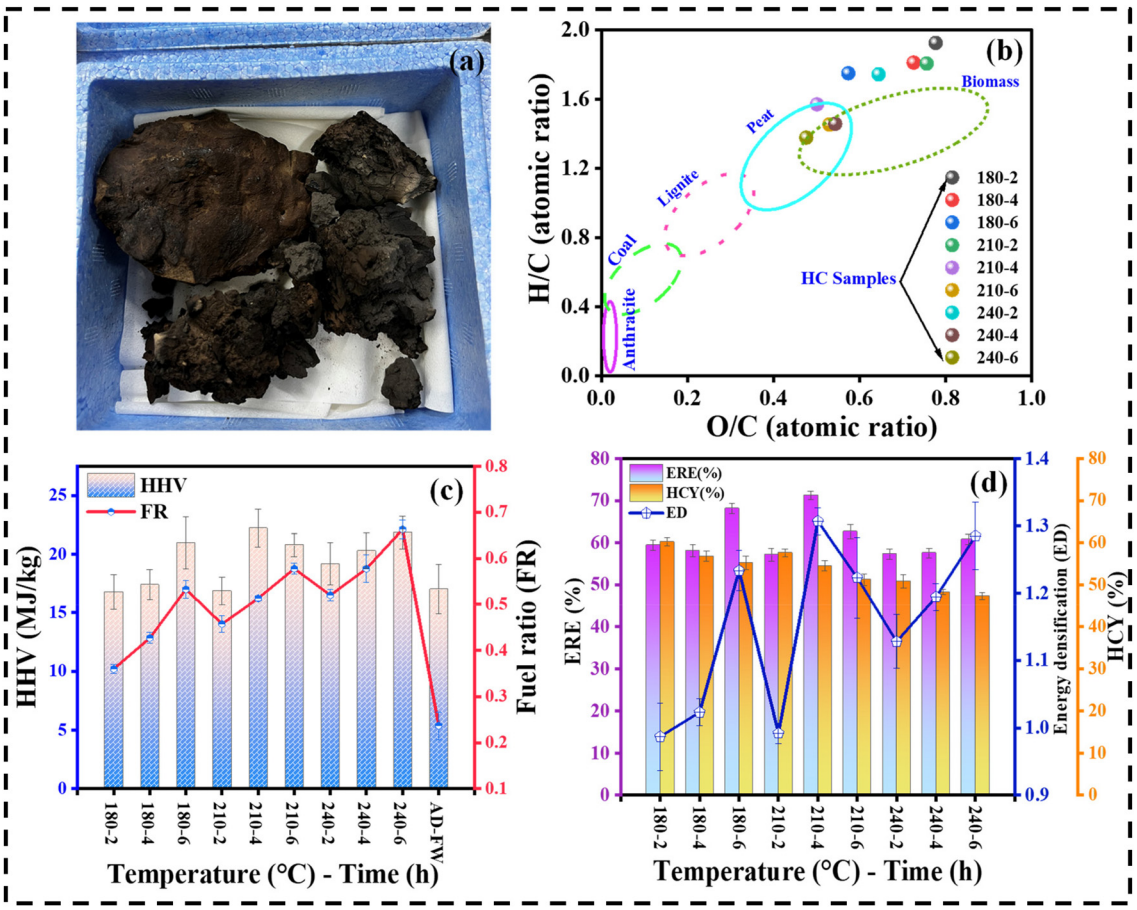

Fig. 2 (a) Resemblance of real HC to lignite coal, (b) Van Krevelen diagram for comparative assessment of intensity of coalification between AD-FW hydrochar and conventional fossil fuel, (c) variation in HHV and FR, (d) variation in ERE, HCY, and energy densification of hydrochar at different HTC temperature (180 °C–240 °C) and time (2 h–4 h).

Further, the HC obtained at 180 °C exhibited H/C and O/C similar to the biomass region (H/C range: 0.94–1.79; O/C range: 0.54–1.23) (Fig. 2b). For information, a wide range of O/C and H/C ratios also reflect the diversity of the biomass in the literature database and are vulnerable due to its biochemical composition.[44] However, with the rise in temperature to 240 °C for an extended HTC reaction duration of 4 h or 6 h the H/C and O/C ratios were analogous to the coalification degree of peat coal region.

A similar trend was also witnessed by Wang *et al.* and Raheem *et al.*[43,45] The FW of plant origin primarily consists of organic matter having hemicellulose, cellulose, lignin, and carbohydrate content. These components undergo degradation at different HTC temperatures and form monomers, oligomers, furans, and phenolic compounds as shown in Table S1.†[46,47] The HTC dissolved products from the aqueous phase undergoes an aromatization reaction onto the HC surface, thereby, enhancing the C content and calorific value of the HC. In summary, both higher HTC temperature and time are crucial for achieving better coalification of AD-FW-derived HC for application as fuel. The similarity of HC to lower-grade coal illustrates its potential as a substitute fuel material and can replace natural fossil fuel to some extent.

The HHV or gross calorific value is an important parameter deployed to analyse the energy content of fuels. Generally, fuels with higher HHV have the advantages of (a) more energy per unit mass, (b) leading to less fuel consumption, (c) being environmentally sustainable as it produces more energy with fewer emissions, (d) proving to be cost-effective fuel, and (e) have better fuel efficiency.[48] The HTC operating condition of 210 °C, and duration of 4 h was found to be the most optimum, resulting in 22.21 MJ kg^{-1} of HHV, (Fig. 2c), *i.e.*, more than the HHVs of HC obtained at other conditions: 16.78 MJ kg^{-1} (180 °C, 2 h); 17.39 MJ kg^{-1} (180 °C, 4 h); 20.96 MJ kg^{-1} (180 °C, 6 h); 16.86 MJ kg^{-1} (210 °C, 2 h); 20.79 MJ kg^{-1} (210 °C, 6 h); 19.17 MJ kg^{-1} (240 °C, 2 h); 20.30 MJ kg^{-1} (240 °C, 4 h); 21.84 MJ kg^{-1} (240 °C, 6 h); and 16.49 MJ kg^{-1} (AD-FW). Similar HHVs were obtained by Gaur *et al.* in the range of 18.25–21.5 MJ kg^{-1} for the HC obtained from sewage sludge (temperature range = 200–300 °C; time = 0.5–2 h).[49] In another investigation, co-HTC of sewage sludge and agro-waste resulted in comparatively lower HHV *i.e.*, 7.65–16.41 MJ kg^{-1} due to the complexity of the precursor.[50] Further, a sudden drop in HHV at other extreme conditions might be due to the breakdown of fatty acids into long-chain hydrocarbons under subcritical process conditions, while glycerol will break down into organic gases, such as methanol and acetaldehyde. Generally, the long-chain fatty acids and glycerol are the hydrolysis products of triglycerides or lipids present in FW, which undergo hydrolysis under high-temperature.[47,51]

Fuel ratio is a key indicator of the burning and combustion characteristics of HC. A higher FR means the fuel has more FC, leading to a slower, more sustained burn, while a lower FR suggests more volatile matter and quicker combustion.[52] For HC, this ratio helps assess its combustion properties compared to other solid fuels like coal or biomass. For the constant retention time of 2 h, the FR reached a maximum of 0.51 at 240 °C, which was 1.46 and 1.13 times higher than at 180 °C and 210 °C, respectively. Thus, it can be concluded that higher retention time enhances the FR and a similar trend was witnessed in terms of reaction time. A shorter retention time resulted in incomplete carbonization reactions and carbon density in HC. The FR reached a maximum of 0.66 for peak operating conditions (240 °C, 6 h), which was 2.87 times higher than the precursor. The reason behind the considerable boost of FR is the corresponding increase in FC and decrease in VS during the severe HTC conditions. The FR of AD-FW-derived HC was found to be similar to the FR of lignite *i.e.*, 0.6 showcasing its aptness as an efficient fuel.

The energy recovery efficiency (ERE) analysis highlights the effectiveness of energy stored in fuel and it is influenced by HCY and HHV. As witnessed the ERE and energy densification (ED) were higher at optimized conditions than the HCY on account of the higher HHV of HC (Fig. 2d). The HCY at the optimum HTC conditions of 210 °C, 4 h was 54.5%; however, the ERE and ED were attaining maxima of 73.41% and 1.34. The above inferences are supported by an investigation conducted on paper mill effluent treatment plant sludge-derived HC having a maximum HHV of 22.25 MJ kg^{-1} and ERE of 75.03%.[53] Hence, the AD-FW-derived HC can be an extraordinary choice for use as a renewable fuel, co-firing material in power plants, or for domestic purposes. As per the Indian Standard (IS 17225), the minimum HHV of renewable solid fuel must be in the range of 14–16.5 MJ kg^{-1}.[54,55] The HC generated from AD-FW successfully met this requirement.

Functional and morphological properties of mesoporous AD-FW hydrochar. The Fourier transform infrared spectroscopy (FTIR) results (Fig. 3a) affirmed the previous hypothesis, that the HC surface is rich in oxygen-containing functional groups (OFGs). The broad band around 3400 cm^{-1} was ascribed to the –OH stretching in all the HC and the raw AD-FW; however, the band becomes flatter with the rise in temperature due to dehydration reactions during HTC. Moreover, the bands at 3000–2800 cm^{-1} (2925 cm^{-1} and 2850 cm^{-1}) were associated with the existence of aliphatic C-CHx and other methylene groups in the HC, respectively.[56] The bands around 1550 cm^{-1} and 1415 cm^{-1} indicate the aromatic C=C and benzene rings formed in the HC during the HTC of D-xylose and cellulose precursors.[57,58] Additionally, the enhanced peaks at 1030 cm^{-1} and 2900 cm^{-1} were related to the aliphatic ether C–O–C stretching vibrations and bending vibrations of the aromatic nucleus C–H bond, due to high carbon aromatization and aldol condensation during HTC of AD-FW.[59] Nonetheless, the signals located in the region 800 cm^{-1} to 400 cm^{-1} were attributed to the existence of siloxane bonds (Si–O–Si).[60] The substantial ash concentration attested to the retention of the mineral components during the HTC process. To summarize, OFGs in fuels can have a variety of consequences on fuel properties. Although they can increase stability, cut emissions, and increase octane and cetane numbers, they can also diminish the calorific value and cause problems with hydrophilicity and corrosion. Fuel com-

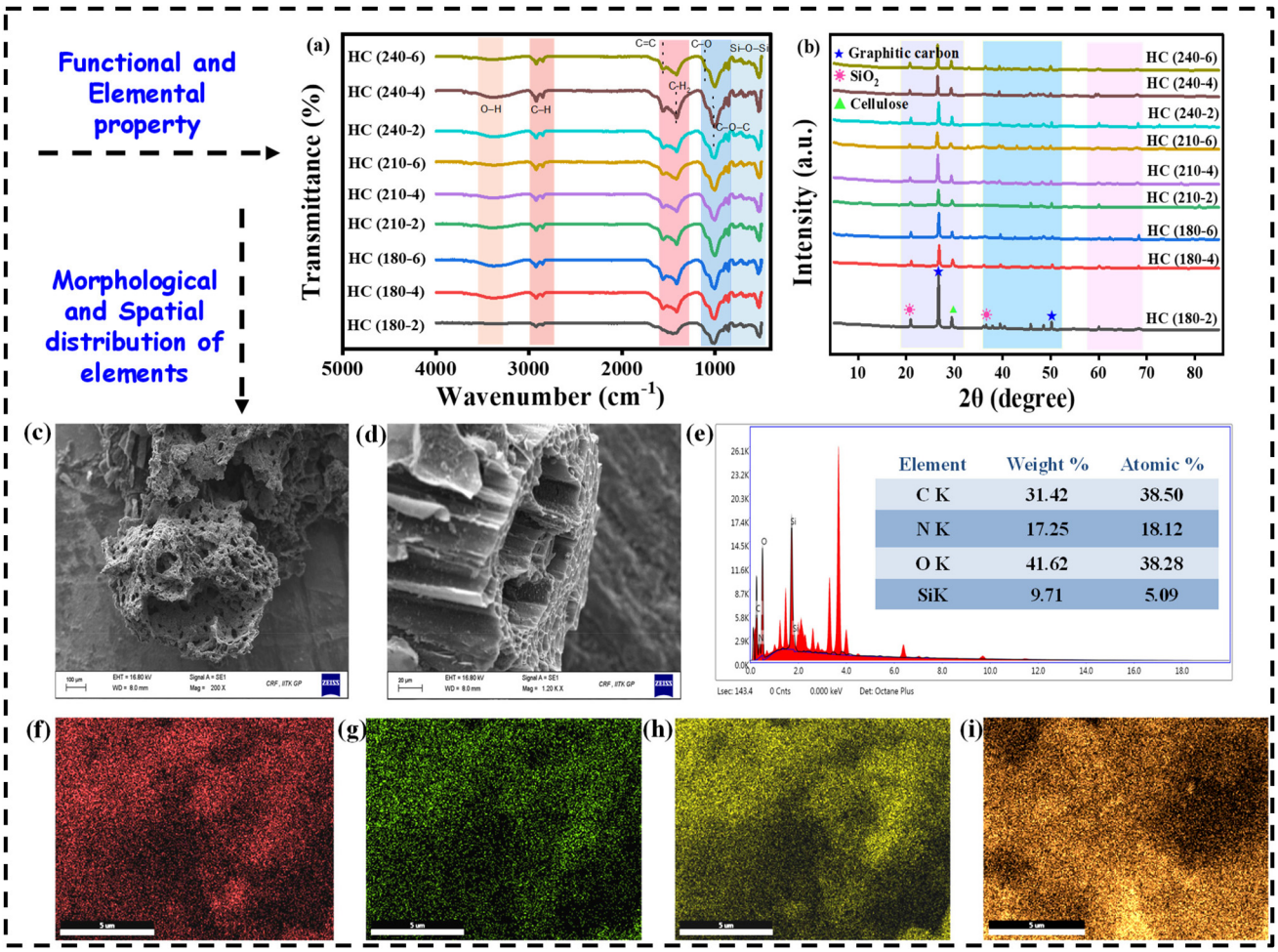

Fig. 3 Functional and elemental characteristics of AD-FW hydrochar by (a) FTIR and (b) XRD analysis, mesoporous structure of AD-FW/HC (c) SEM (200×), (d) SEM 1.20 K×, (e) EDX plot, (f–i) elemental mapping of C, Si, N, and O, respectively (Fig. S2,† enlarged view of FTIR analysis).

position and careful consideration of the kind and quantity of oxygenates are necessary to counteract these effects and provide fuels that satisfy the demands of various applications.[61]

Besides, the X-ray diffraction (XRD) analysis (Fig. 3b) showed distinct diffraction peaks at 26.4° and 50.1° with crystalline plane (002) and (102) might correspond to the presence of aromatic carbon rings formed during the hydrothermal process and are stacked in a pattern similar to the graphite. However, the precursor for HC synthesis is FW + UASBR sludge, both are real-field waste and might contain some external compounds such as silica or clay-based minerals having similar diffraction patterns.[62,63] Moreover, a standardised peak of cellulose at 30° corresponding to the plane (040) was observed signifying the incomplete degradation of cellulose during the HTC process.[64] However, due to the presence of inorganic minerals, certain peaks of SiO_2 were observed at 20.8° and 36.6°, supporting the results obtained in FTIR analysis.[62,65]

Further, the surface morphology of the HC synthesized at optimized conditions (210 °C, 4 h), analysed using scanning electron microscopy (SEM), revealed the existence of rough surfaces, small voids, and holes. This suggests the existence of a linked porous network of surfaces.[53] These rough surface (Fig. 3c) forms were easily seen in the micrographs and were also reported by Gai *et al.* for sewage sludge-derived HC.[66] The second micrograph (Fig. 3d) displayed the intactness of the plant cellular structure with more pores and long channels, affirming the generation of bio-coal from biomass of plant origin. Generally, a well-developed porous structure of HC makes the reactant transportation to active areas and reaction product removal, which promotes effective gasification or combustion processes.[67] Further, the SEM energy dispersive X-ray (EDX) elemental mapping confirmed the presence of C, N, O, and Si, in the as-synthesized HC (Fig. 3e–i).

Combustion and thermogravimetric characteristics of AD-FW hydrochar. The combustion profile of the AD-FW/HC (210 °C, 4 h) was established using the differential thermogravimetric analysis – differential thermal analysis (DTG-DTA) (Fig. 4a and b). The results indicated that the combustion of AD-FW/HC occurred in three major phases. During the preheating phase, a slight weight loss in the temperature range of

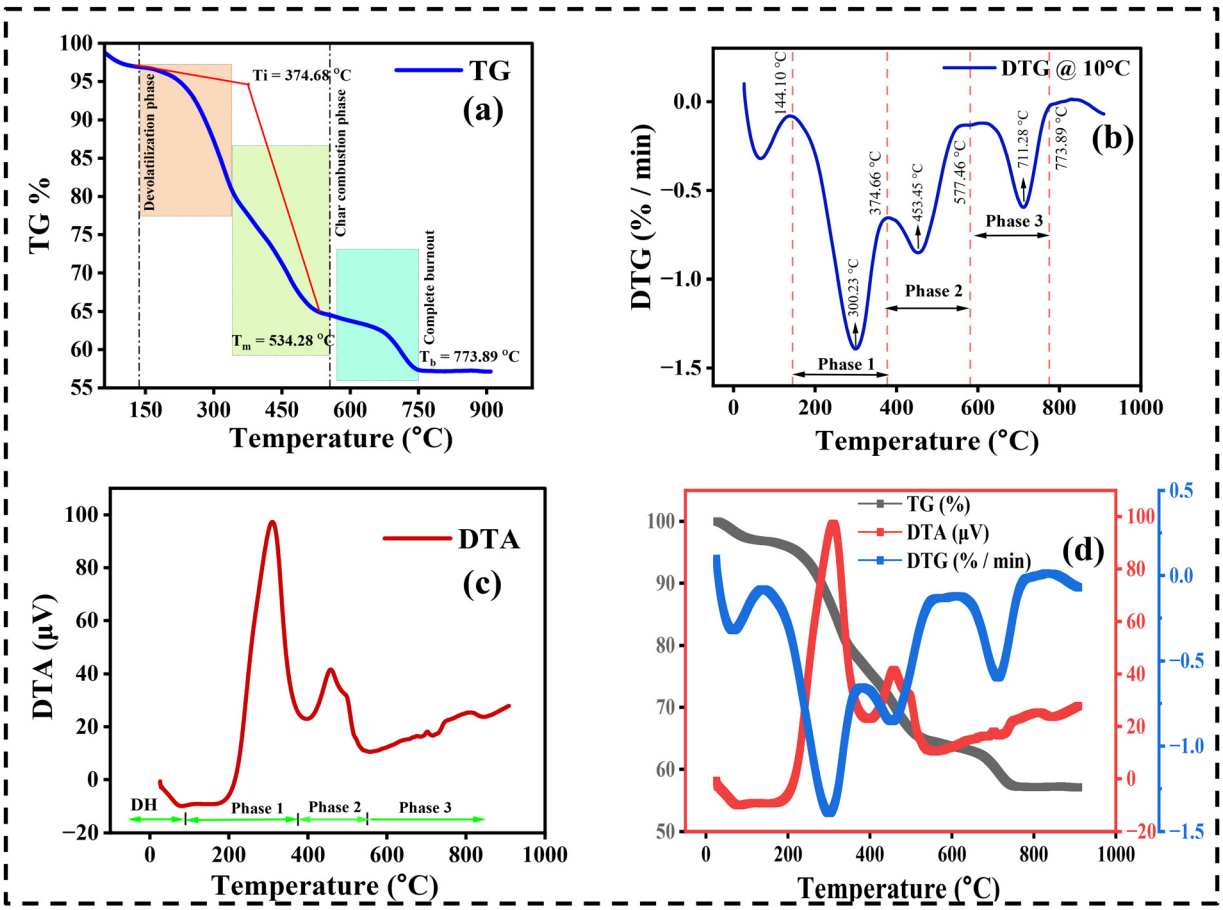

Fig. 4 Combustion profile of AD-FW/HC (a) TG %, (b) DTG % min^{-1}, (c) DTA (µV), and (d) combined combustion profile.

30–150 °C was due to evaporation of water. Subsequently, the initial weight loss in the region below 144 °C resulted from the dehydration of HC *i.e.*, removal of chemically bonded water molecules. The first combustion phase occurred in the temperature range of 144.46–374.46 °C, which was linked to the devolatilization of VS leading to the formation of char.[68]

The weight loss in the first phase can also be attributed to the decomposition of hemicellulose and cellulose content. Further, the second combustion phase (temperature range 374.46–577.46 °C) was attributed to the oxidation of solid carbonaceous material (char) along with the oxidation of residual VS. The third phase led to the complete burnout of the solid material. Further, bond breaking occurs, and the evolution of organic matter as tar, gases, and condensation reactions also takes place in this region. For comparative assessment of the combustion behaviour of AD-FW/HC with other fossil fuels (anthracite, bituminous, lignite, and peat), the ignition temperature (T_i), maximum combustion temperature (T_m), and burnout temperature were determined (T_b). The T_i of the AD-FW/HC *i.e.*, 374.68 °C was in good agreement with the reported T_i values of lignite (300–400 °C), bituminous coal (400–550 °C), and anthracite bituminous coal (550–700 °C).[69] A higher T_i value indicates strong combustion efficiency, which allows safe fuel transportation, and minimizes the risk of potential fire or explosion.[70] Further, the T_m, T_b, and the maximum rate of VS combustion were 534.28 °C, 773.89 °C, and −1.34% min^{-1} interpreting the thermal stability of fuel as the fuel will take longer time to complete burnout. The extraordinary fuel performance of AD-FW/HC might be due to reduced VS as the fuel with high VS burned with inadequate air supply, pose a pollution risk by generating dark smoke and experiencing low combustion efficiency due to heat loss.[71] Furthermore, in DTA analysis (Fig. 4c and d), the peak around 100 °C corresponds to dehydration and volatilization of small organic molecules. The exothermic peaks in Phase 1 and Phase 2 were attributed to the degradation of hemicellulose and cellulose content during the thermal treatment. Followed by the decomposition of the lignin content in Phase 3.[72]

Resource 3: bioelectricity potential of HTC-PW fed MFC

As the downstream processing, the HTC-PW was treated using the MFC technology (Fig. 5a) for abatement of organics and bioelectricity production at the same time. The HTC-PW was characterized to have an initial chemical oxygen demand (COD) of 24 000 ± 5000 mg L^{-1}, acetate ions concentration of 12480 ± 3000 mg L^{-1}, and pH of 6.6. However, it undergoes a dilution process, reducing the initial COD concentration to 6000 mg L^{-1} for utilization as substrate in MFC. Dilution was

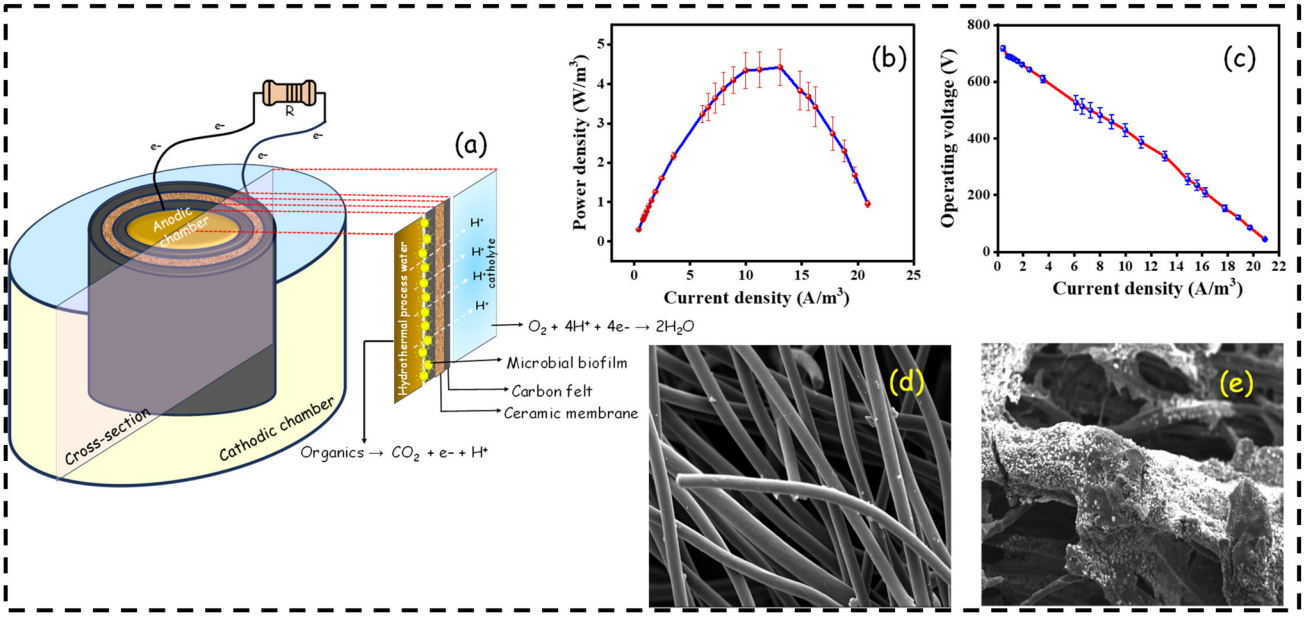

Fig. 5 Illustration of (a) functioning of MFC, (b) power generation of fed batch mode MFC with HTC-PW, (c) polarisation curve, (d) SEM of bare carbon felt, (e) SEM image of microbial film developed in the anodic film of HTC-PW/MFC.

done to prevent shock loading and acclimatization of HTC-PW-specific exoelectrogens in the anodic chamber of MFC. Following a 20-day acclimatization period, a noteworthy COD removal of 76.0 ± 4.6% was observed. Additionally, the system was able to achieve coulombic efficiency and maximum power density of 19.9 ± 2.4% and 4.41 ± 0.64 W m^{-3} (Fig. 5b and c), respectively. The efficient performance of HTC-PW-fed MFC might be due to the high proliferation of electrogenic microorganisms in adverse environments (Fig. 5d and e). Also, the presence of furans and phenolic compounds in the HTC-PW inhibits the methanogenesis process in the MFC and enhances the electron's availability for better power output.[73,74] The above-mentioned results were comparable to other investigations conducted by Das *et al.* and Chakraborty *et al.* on the synthetic media (COD ~ 3000 mg L^{-1}) and achieved organics abatement efficiency of 63.3 ± 1.8% and 73.5 ± 9.1% respectively.[75,76]

Further, to determine the organic species abatement during the process, the total organic carbon (TOC) content was analysed. The TOC content of HTC-PW, before and after treatment in the MFC was found to be 2395 ± 5 mg L^{-1} and 1028 ± 3 mg L^{-1}, respectively, *i.e.*, approx. 57% of TOC removal was achieved. The reason behind the limited performance of MFC towards TOC degradation is the presence of phenolic, aromatics, and recalcitrant organic compounds in HTC-PW. In conclusion, this investigation affirms the effectiveness of the MFC in treating complex wastewater *i.e.*, HTC-PW, demonstrating substantial COD removal and outperforming other substrates in terms of coulombic efficiency and power density. However, the optimization of HTC process conditions, use of cathode catalyst, and careful selection of microbial community might further enhance the performance of the MFC in the future.

Microbial dynamics of the anodic biofilm. The present investigation deployed acetate-rich HTC-PW as the substrate for MFC and metagenomic analysis of the microbial community developed on anode (biofilm) was performed. The higher coulombic performance in HTC-PW/MFC might be attributed to the most easy-to-degrade substrate acetate in HTC-PW for exo-electrogenic bacteria. Metagenomic studies help to identify novel electroactive microorganisms and their associated genes, contributing to better performance of MFC in the case of complex substrates like HTC-PW. The genus level results revealed the existence of *Clostridium* (~57.5%) bacterial group, followed by *Treponema* (~18.5%), *Blattabacterium* (~5.05%), *Flavobacterium* (~3.56%), *Desulfallas* (~3.25%), *Sorangium* (~2.54%), and *Eggerthella* (~2.47%) in the biofilm developed (Fig. S3†). These microbes proliferate mostly in low pH, strictly anaerobic conditions, and might play significant role in electricity generation (are exoelectrogens). According to previous investigations, direct electron transfer was reportedly carried out by membrane-bound cytochromes found in *Clostridium butyricum*. This vast genus of obligate anaerobe bacteria, *Clostridium* is a member of the Firmicutes phylum. Hence, the genus-level distributions also complement the results observed at phylum-level distributions having dominant phyla of Firmicutes, Proteobacteria, Bacteroidetes, Spirochaetes, and Actinobacteria. On the other hand, the most commonly utilized substrate glucose and sucrose, exhibited microbial diversity, with *Bacilli* dominating the biofilm (33.3%), followed by *Bacteroidetes* (16.7%), *Clostridia* (16.7%), *Betaproteobacteria* (16.7%), and *Deltaproteobacteria* as per the literature. Conversely, the suspended community was primarily comprised of *Deltaproteobacteria* (33.3%) and *Betaproteobacteria* (33.3%), with lesser proportions of *Bacteroidetes* (16.7%) and

Bacilli.[77,78] However, the above-mentioned literature is highly contradictory to the observed results in the present investigation. Table S2† represent the major electroactive communities with their potential role in treating the HTC-PW and bioelectricity generation. As discussed, the most common species found in these bands seem to share evolutionary relationships (>99% similarity) with the Firmicutes family's Bacilli and Clostridia. It has been suggested that one of the functions of Firmicutes may be the conversion of fermentable substrates (glucose and propionate) into simple organic compounds.[77] Following the addition of acetate, biofilm and suspended communities containing deltaproteobacteria and gamma proteobacteria were discovered, indicating that certain electrochemically active bacteria were enhanced following the transition to acetate. The primary bacterial family found in acetate-enriched MFCs has been identified as deltaproteobacteria, which is thought to be in charge of the direct electron transport to the electrode. The electron transfer mechanism is particularly significant for MFC technology, which enhances performance of system.[79] Therefore, the present metagenomic analysis support the extraordinary performance of MFC fed with highly adverse real wastewater (HTC-PW) with a diverse array of electrogens that contributed to higher power production during the treatment process.

Comparative environmental impact assessment

The LCA was performed based on the data inventory (Table S3†) prepared using the lab-scale experimental set-up, considering only the operational requirements. For the present investigation, the material and capital costs are ignored as they will show great uncertainty, and probably not replicate the real field condition.[80] The selected midpoint and endpoint impact categories and their respective units are enlisted in Table 2. Based on the midpoint characterisation, the impacts of AD, AD + HTC, and AD + HTC + MFC on the environment are stipulated in Fig. 6a–c, respectively. The integration of AD with HTC was found to have less environmentally negative impacts in the category of GW, SOD, OFDD, FPMF, TA, ME, HCT, and HNCT (abbreviations provided in Table 2). Similar results were obtained by Zhao *et al.* on integrating AD with HTC because of the stabilisation of carbon in the form of HC resulting in a positive environmental impact.[81] Otherwise, the open dumping of digestate resulting from AD would have greenhouse gas emissions and cause serious environmental threats. All the three technologies have environmental gain in the FRS category *i.e.*, -2.80×10^{-4}, -2.95×10^{-5}, and -2.62×10^{-4} kg oil, *e.g.*, for AD, AD + HTC, AD + HTC + MFC, due to recovery of biomethane, HC, and bioelectricity.

Later, integration of MFC technology, for the treatment of HTC-PW, served an additional benefit on a much larger scale in the category of FE with impact value significantly reduced to -3.60×10^{-7} kg P eq. from 7.09×10^{-7} kg P eq. (for AD + HTC). Moreover, the integrated system also has a minimal negative impact in the category of TE *i.e.*, 2.03×10^{-4} kg 1,4-DCB, compared to AD (2.16×10^{-4} kg 1,4-DCB) and AD + HTC (0.000145972 kg 1,4-DCB). The reasons behind the lesser ecotoxicity on the terrestrial environment were the resources recovered during the process. Further, assessing the endpoint damage (based on single score) of AD + HTC + MFC resulted in the least impact on human health (37.17 μPt), ecosystem (−123.30 μPt), and resources (−3.33191 μPt) compared to AD + HTC and AD (Fig. 6d).

For AD + HTC and AD, the individual scores recorded in the categories of human health were 37.39 μPt and 73.27 μPt, respectively. In terms of the ecosystem, the scores were 2.05 μPt and 4.40 μPt, respectively. Whereas as, for resources, the scores observed were −3.33 μPt for AD + HTC and −1.76 μPt for AD. Further, for the mass balance analysis, the

Table 2 Environment impact categories based on ReCiPe 2016

	Impact category	Abbreviation	Unit
Midpoint	Global warming potential	GW	kg CO_2 eq.
	Stratospheric ozone depletion potential	SODP	kg CFC11 eq.
	Ionizing radiation potential	IRP	kBq Co-60 eq.
	Ozone formation, human health potential	OFHH	NO_x eq.
	Fine particulate matter formation potential	FPMF	kg PM2.5 eq.
	Ozone formation, terrestrial ecosystems potential	OFTEP	kg NO_x eq.
	Terrestrial acidification potential	TA	SO_2 eq.
	Freshwater eutrophication potential	FE	kg P eq.
	Marine eutrophication potential	ME	kg N eq.
	Terrestrial ecotoxicity potential	TET	kg 1,4-DCB
	Freshwater ecotoxicity potential	FEc	kg 1,4-DCB
	Marine ecotoxicity potential	MET	kg 1,4-DCB
	Human carcinogenic toxicity potential	HCT	kg 1,4-DCB
	Human non-carcinogenic toxicity potential	HNCT	1,4-DCB
	Land use potential	LU	m^2 a crop eq.
	Mineral resource scarcity potential	MRS	$\times 10^{-2}$ kg Cu eq.
	Fossil resource scarcity potential	FRS	kg oil eq.
	Water consumption potential	WC	m^3
Endpoint	Human health		DALY
	Ecosystems		Species. year
	Resources		USD 2013

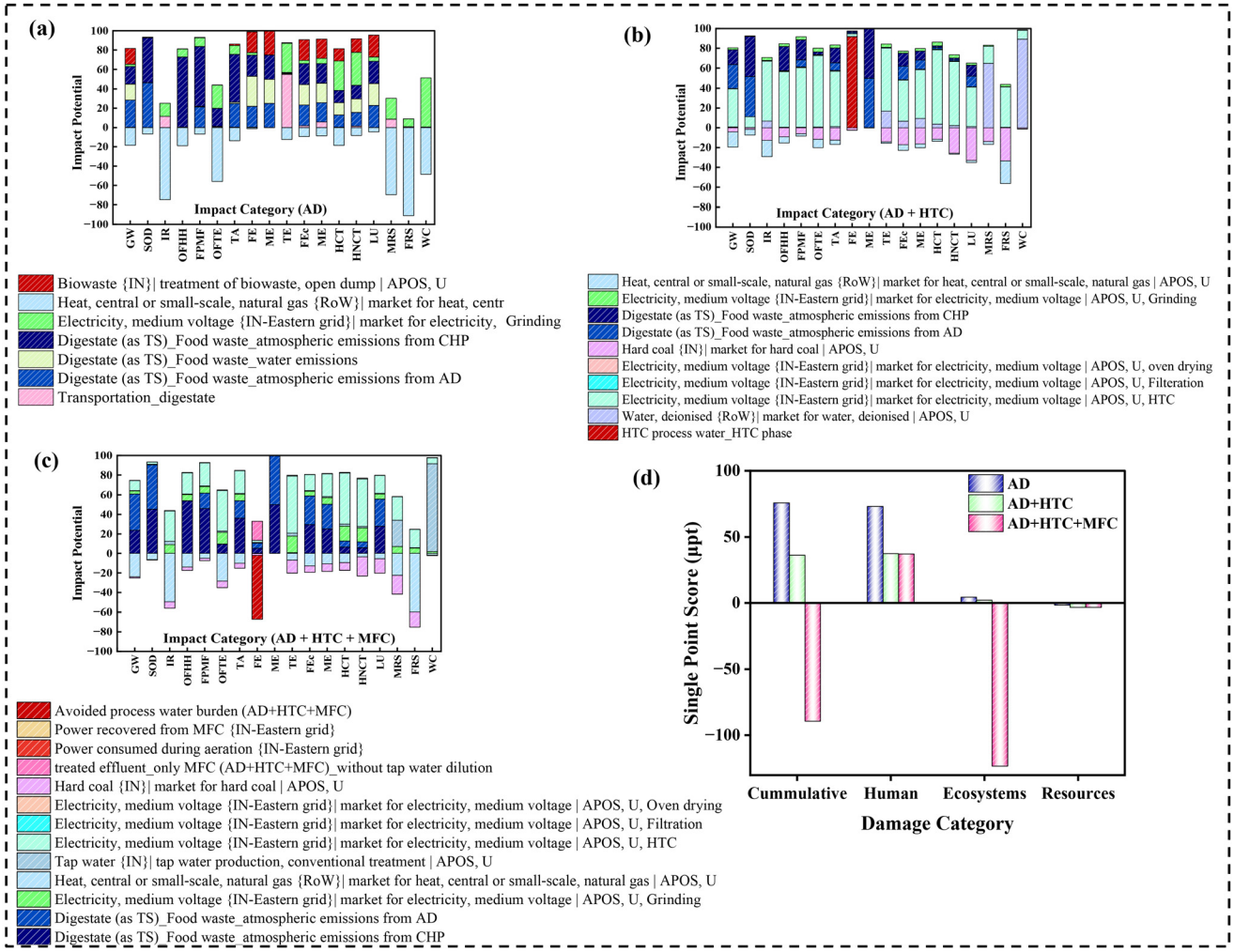

Fig. 6 Mid-point impact assessment of (a) AD, (b) AD + HTC, (c) AD + HTC + MFC, and (d) comparative end-point damage assessment (single score).

1 kg of precursor (FW slurry + UASBR sludge) containing 210 g of VS is considered, which is subjected to the integrated technology *i.e.*, AD + HTC + MFC. The results of mass and energy balance showed effective VS treatment with net energy gain in the process (Fig. S5†). Therefore, it can be concluded that the integration of three technologies for FW treatment is beneficial as it reduces the load on natural resources; however, it can have environmentally negative impacts in terms of electricity requirements, emissions, and water consumption at the scale of the present investigation. However, operation at a larger scale and high magnitude of resource recovery may compensate for the cost of external energy consumed and can be a cutting-edge solution to waste management.

Conclusion

From the above-detailed investigation, it can be concluded that the bottleneck of the AD technology for FW management, has been ameliorated by adopting HTC technology for digestate valorisation. By adopting HTC, the digestate can be successfully transformed to HC, and have the highest intensity of coalification at an optimized operating temperature of 210 °C and reaction time of 4 h. Further, the generated HC has a distinct calorific value similar to lignite coal, and similar physiochemical, and fuel characteristics, showcasing its potential to replace fossil fuels to some extent. Meanwhile, the highly complex end product HTC-PW was effectively treated using the MFC technology achieving ~76% abatement of organic content. Further, it generated bioelectricity, which adds to the resource recovery statistics of the integrated process (AD + HTC + MFC). The metagenomic analysis revealed the abundance of strict anaerobes *Clostridium*, *Treponema*, and *Blattabacterium* in the anodic biofilm of the HTC-PW-MFC. The presence of such electro-active microbes justified the higher power output from the HTC-PW even in the absence of a cathode catalyst. However, power production can be enhanced by incorporating suitable cathode catalysts and reactor modifications in future.

Ultimately, the comparative LCA of AD, AD + HTC, and AD + HTC + MFC, revealed the lowest impact of the integrated technology on the environment in terms of resource scarcity (-2.62×10^{-4} kg oil eq.) and freshwater eutrophication (-3.60×10^{-7} kg P eq.). Further, the energy-intensive process can be optimized to cut back the negative environmental impacts of incorporating three technologies. All inclusive, it can be affirmed that adopting HTC for digestate valorisation curtailed the negative emissions of open dumping or landfilling, thereby, reducing environmental pollution. Additionally, this integrated scheme and generation of bio-products with high market value supports the idea of a circular economy, zero-waste to landfill, green technology for wastewater treatment, and sustainable development.

Broader context and environmental implications

Anaerobic digestion is a widely used technology for FW management, however it frequently encounters challenges related to the proper handling of digestate. The unscientific management and land applications of anaerobic digestate are associated with serious environmental issues such as eutrophication, nutrient imbalance, soil acidification, ammonia volatilization, and fugitive greenhouse gas emissions. Simply directing digestate to compost production does not address the growing energy demand and it is unlikely to gain substantial commercial interest.

Integrating HTC technology into the process offers a solution by transforming the digestate into HC, a carbon-rich material with a high calorific value (22.21 MJ kg^{-1}). The HTC operates under subcritical water conditions, eliminating the need for energy-intensive drying. The HC produced can serve as a renewable solid biofuel, offering a partial substitute for fossil fuels. Beyond its role as biofuel, HC can be utilized as a catalyst support or adsorbent in advanced water/wastewater treatment processes.

However, a key limitation of HTC is the generation of HTC-PW that is rich in organic contaminants. This issue can be addressed through the application of an MFC, a bio-electrochemical system that transforms the chemical energy stored in organic matter into electricity while simultaneously reducing the organic load in the HTC-PW. In this study, the MFC achieved a power density of 4.41 W m^{-3}. Notably, for the first time, HTC-PW was treated by deploying MFC embedded with a ceramic-based proton exchange membrane.

Further, the detailed analysis of the microbial proliferation provides future scope for the anodic modifications in the system using enriched culture or by adopting a cathode catalyst. Furthermore, the life cycle assessment proves the positive environmental impacts of downstream augmentation of HTC and MFC, with AD. Thus, the present investigation can help in solving the global issues of food waste management, digestate management, renewable resource recovery, wastewater treatment, and landfill emissions by offering a sustainable approach. Additionally, the recovery of valuables in the form of biomethane, bio-coal, and bioelectricity, attracts the global market and contributes to a circular bio-economy.

Author contributions

S. Y. conceptualised the research work, performed experiments, and wrote the original manuscript. M. M. D. conducted the experiments and co-wrote the manuscript. M. M. G. provided the funding to conduct the experimental work, administered the project, supervised, and reviewed the manuscript. B. K. D. supervised, validated, reviewed, and edited the manuscript. All the authors contributed to the discussion of experimental results and reviewed the manuscript.

Data availability

The data supporting this article including materials and methods have been included as part of the ESI.†

Conflicts of interest

The authors affirm that they have no known financial or interpersonal conflicts that would have an impact on the research work presented in this paper.

Acknowledgements

The authors acknowledge the Department of Science and Technology, Ministry of Science and Technology, Government of India, for providing financial assistance to this research project (File No. DST/IMRCD/India-EU/Watercall2/SARASWATI2.0/2018).

References

1 D. S. Gunarathne, I. A. Udugama, S. Jayawardena, K. V. Gernaey, S. S. Mansouri and M. Narayana, *Sustain. Prod. Consum.*, 2019, **17**, 196–214.
2 E. Iacovidou, C. A. Velis, P. Purnell, O. Zwirner, A. Brown, J. Hahladakis, J. Millward-Hopkins and P. T. Williams, *J. Cleaner Prod.*, 2017, **166**, 910–938.
3 T. E. T. Dantas, E. D. de-Souza, I. R. Destro, G. Hammes, C. M. T. Rodriguez and S. R. Soares, *Sustain. Prod. Consum.*, 2021, **26**, 213–227.
4 I. A. Udugama, L. A. H. Petersen, F. C. Falco, H. Junicke, A. Mitic, X. F. Alsina, S. S. Mansouri and K. V. Gernaey, *Food Bioprod. Process.*, 2020, **119**, 133–147.
5 R. Ravindran and A. K. Jaiswal, *Trends Biotechnol.*, 2016, **34**, 58–69.

6 C. Negri, M. Ricci, M. Zilio, G. D'Imporzano, W. Qiao, R. Dong and F. Adani, *Renewable Sustainable Energy Rev.*, 2020, **133**, 110138.
7 Z. Yang, Y. Liu, J. Zhang, K. Mao, M. Kurbonova, G. Liu, R. Zhang and W. Wang, *J. Cleaner Prod.*, 2020, **256**, 120594.
8 K. Izumi, Y. K. Okishio, N. Nagao, C. Niwa, S. Yamamoto and T. Toda, *Int. Biodeterior. Biodegrad.*, 2010, **64**, 601–608.
9 L. R. Lynd, G. T. Beckham, A. M. Guss, L. N. Jayakody, E. M. Karp, C. Maranas, R. L. McCormick, D. Amador-Noguez, Y. J. Bomble, B. H. Davison, C. Foster, M. E. Himmel, E. K. Holwerda, M. S. Laser, C. Y. Ng, D. G. Olson, Y. Román-Leshkov, C. T. Trinh, G. A. Tuskan, V. Upadhayay, D. R. Vardon, L. Wang and C. E. Wyman, *Energy Environ. Sci.*, 2022, **15**, 938–990.
10 M. Kiehbadroudinezhad, A. Merabet, C. Ghenai, A. G. Abo-Khalil and T. Salameh, *Heliyon*, 2023, **9**, e13407.
11 T. Spencer, *Clean Energy Market Monitor*, IEA, Paris, 2024.
12 IEA, *Tracking Clean Energy Progress*, Paris, 2023.
13 Y. Ren, M. Yu, C. Wu, Q. Wang, M. Gao, Q. Huang and Y. Liu, *Bioresour. Technol.*, 2018, **247**, 1069–1076.
14 S. Song, J. W. Lim, J. T. E. Lee, J. C. Cheong, S. H. Hoy, Q. Hu, J. K. N. Tan, Z. Chiam, S. Arora, T. Q. H. Lum, E. Y. Lim, C. H. Wang, H. T. W. Tan and Y. W. Tong, *Waste Manage.*, 2021, **136**, 143–152.
15 M. Yan, F. Chen, T. Li, L. Zhong, H. Feng, Z. Xu, D. Hantoko and H. Wibowo, *Process Saf. Environ. Prot.*, 2023, **178**, 296–308.
16 S. Dutta, M. He, X. Xiong and D. C. W. Tsang, *Bioresour. Technol.*, 2021, **341**, 125915.
17 L. I. Fuldauer, B. M. Parker, R. Yaman and A. Borrion, *J. Cleaner Prod.*, 2018, **185**, 929–940.
18 F. Monlau, C. Sambusiti, E. Ficara, A. Aboulkas, A. Barakat and H. Carrère, *Energy Environ. Sci.*, 2015, **8**, 2600–2621.
19 J. Mumme, L. Eckervogt, J. Pielert, M. Diakité, F. Rupp and J. Kern, *Bioresour. Technol.*, 2011, **102**, 9255–9260.
20 M. M. Titirici, R. J. White, C. Falco and M. Sevilla, *Energy Environ. Sci.*, 2012, **5**, 6796–6822.
21 M. Pecchi and M. Baratieri, *Renewable Sustainable Energy Rev.*, 2019, **105**, 462–475.
22 L. Wang, A. Li and Y. Chang, *Water Res.*, 2017, **112**, 72–82.
23 Z. Liu, D. Ma, L. Liang, X. Hu, M. Ling, Z. Zhou, L. Fu, Z. Liu and Q. Feng, *Process Saf. Environ. Prot.*, 2022, **161**, 88–99.
24 H. B. Sharma, S. Panigrahi, A. K. Sarmah and B. K. Dubey, *Sci. Total Environ.*, 2020, **706**, 135907.
25 Q. Lang, H. Luo, Y. Li, D. Li, Z. Liu and T. Yang, *Sustainable Energy Fuels*, 2019, **3**, 2329–2336.
26 H. S. Kambo, J. Minaret and A. Dutta, *Waste Biomass Valorization*, 2018, **9**, 1181–1189.
27 E. Erdogan, B. Atila, J. Mumme, M. T. Reza, A. Toptas, M. Elibol and J. Yanik, *Bioresour. Technol.*, 2015, **196**, 35–42.
28 P. Pandey, V. N. Shinde, R. L. Deopurkar, S. P. Kale, S. A. Patil and D. Pant, *Appl. Energy*, 2016, **168**, 706–723.
29 F. Guo, G. Fu, Z. Zhang and C. Zhang, *Bioresour. Technol.*, 2013, **136**, 425–430.
30 C. K. Sakdaronnarong, S. Thanosawan, S. Chaithong, N. Sinbuathong and C. Jeraputra, *Fuel*, 2013, **107**, 382–386.
31 H. J. Mansoorian, A. H. Mahvi, A. J. Jafari and N. Khanjani, *J. Saudi Chem. Soc.*, 2016, **20**, 88–100.
32 Q. Wen, Y. Wu, L. Zhao and Q. Sun, *Fuel*, 2010, **89**, 1381–1385.
33 X. Dai, N. Duan, B. Dong and L. Dai, *Waste Manage.*, 2013, **33**, 308–316.
34 M. S. Prabhu and S. Mutnuri, *Waste Manage. Res.*, 2016, **34**, 307–315.
35 V. Cabbai, M. Ballico, E. Aneggi and D. Goi, *Waste Manage.*, 2013, **33**, 1626–1632.
36 M. T. Reza, J. Mumme and A. Ebert, *Biomass Convers. Biorefin.*, 2015, **5**, 425–435.
37 S. Wu, Q. Wang, M. Fang, D. Wu, D. Cui, S. Pan, J. Bai, F. Xu and Z. Wang, *Sci. Total Environ.*, 2023, **897**, 165327.
38 P. Gao, Y. Zhou, F. Meng, Y. Zhang, Z. Liu, W. Zhang and G. Xue, *Energy*, 2016, **97**, 238–245.
39 X. Zhang, L. Zhang and A. Li, *J. Environ. Manage.*, 2017, **201**, 52–62.
40 K. Rathika, S. Kumar and B. R. Yadav, *Sci. Total Environ.*, 2024, **906**, 167828.
41 M. Malhotra and A. Garg, *Waste Manage.*, 2020, **117**, 114–123.
42 L. Leng, L. Yang, S. Leng, W. Zhang, Y. Zhou, H. Peng, H. Li, Y. Hu, S. Jiang and H. Li, *Sci. Total Environ.*, 2021, **756**, 143679.
43 A. Raheem, Q. He, L. Ding, W. Dastyar and G. Yu, *J. Cleaner Prod.*, 2022, **338**, 130578.
44 Y. Chen, Z. Wang, S. Lin, Y. Qin and X. Huang, *Cleaner Mater.*, 2023, **9**, 100206.
45 G. Wang, J. Zhang, J. Y. Lee, X. Mao, L. Ye, W. Xu, X. Ning, N. Zhang, H. Teng and C. Wang, *Appl. Energy*, 2020, **266**, 114818.
46 H. B. Sharma, S. Panigrahi and B. K. Dubey, *Bioresour. Technol.*, 2021, **333**, 125187.
47 C. Zheng, X. Ma, Z. Yao and X. Chen, *Bioresour. Technol.*, 2019, **285**, 121347.
48 B. Song and P. Hall, *Front. Energy Res.*, 2020, **8**, 1–7.
49 R. Z. Gaur, O. Khoury, M. Zohar, E. Poverenov, R. Darzi, Y. Laor and R. Posmanik, *Energy Convers. Manage.*, 2020, **224**, 113353.
50 S. Zhang, M. Pi, Y. Su, D. Xu, Y. Xiong and H. Zhang, *Biomass Bioenergy*, 2020, **140**, 105664.
51 W. Bühler, E. Dinjus, H. J. Ederer, A. Kruse and C. Mas, *J. Supercrit. Fluids*, 2002, **22**, 37–53.
52 S. Wu, Q. Wang, D. Cui, H. Sun, H. Yin, F. Xu and Z. Wang, *J. Energy Inst.*, 2023, **108**, 101209.
53 S. Oumabady, S. P. Sebastian, S. P. B. Kamaludeen, M. Ramasamy, P. Kalaiselvi and E. Parameswari, *Sci. Rep.*, 2020, **10**, 1–12.
54 J. Lee, K. Lee, D. Sohn, Y. M. Kim and K. Y. Park, *Energy*, 2018, **153**, 913–920.
55 Indian Standards17225-1, *2020(FDIS), Solid biofuels—Fuel specifications and classes—Part 1: General requirements*, 2020, vol. 2020.
56 M. Asadieraghi and W. M. A. W. Daud, *Energy Convers. Manage.*, 2014, **82**, 71–82.

57 C. Goel, S. Mohan, P. Dinesha and M. A. Rosen, *Chem. Pap.*, 2024, **78**, 3845–3856.
58 S. Guo, X. Dong, T. Wu, F. Shi and C. Zhu, *J. Anal. Appl. Pyrolysis*, 2015, **116**, 1–9.
59 J. H. Zhang, Q. M. Lin and X. R. Zhao, *J. Integr. Agric.*, 2014, **13**, 471–482.
60 Y. Gao, X. Wang, J. Wang, X. Li, J. Cheng, H. Yang and H. Chen, *Energy*, 2013, **58**, 376–383.
61 M. A. Nemitallah, M. A. Habib and H. M. Badr, *Arch. Thermodyn.*, 2017, **41**, 1670–1708.
62 L. Wang, K. Lü, Y. Chang, X. Cao and Q. Huo, *J. Environ. Manage.*, 2023, **326**, 116841.
63 D. Tharani and M. Ananthasubramanian, *Biomass Convers. Biorefin.*, 2024, **14**, 12517–12529.
64 I. Akkari, L. Spessato, Z. Graba, N. Bezzi and M. M. Kaci, *Sustainable Chem. Pharm.*, 2023, **31**, 100924.
65 J. Liu, L. Yang, E. Shuang, C. Jin, C. Gong, K. Sheng and X. Zhang, *Fuel*, 2022, **315**, 123172.
66 C. Gai, Y. Guo, T. Liu, N. Peng and Z. Liu, *Int. J. Hydrogen Energy*, 2016, **41**, 3363–3372.
67 X. Zhuang, Y. Song, H. Zhan, X. Yin and C. Wu, *Fuel*, 2020, **260**, 116320.
68 Z. Zhang, J. Yang, J. Qian, Y. Zhao, T. Wang and Y. Zhai, *Bioresour. Technol.*, 2021, **324**, 124686.
69 H. Su, X. Zhou, R. Zheng, Z. Zhou, Y. Zhang, G. Zhu, C. Yu, D. Hantoko and M. Yan, *Sci. Total Environ.*, 2021, **754**, 142192.
70 P. Basu, *Biomass Characteristics*, Elsevier Inc., 2013.
71 F. Liu, R. Yu, X. Ji and M. Guo, *Bioresour. Technol.*, 2018, **263**, 508–516.
72 J. Petrović, N. Perišić, J. D. Maksimović, V. Maksimović, M. Kragović, M. Stojanović, M. Laušević and M. Mihajlović, *J. Anal. Appl. Pyrolysis*, 2016, **118**, 267–277.
73 F. Wang, W. Yi, D. Zhang, Y. Liu, X. Shen and Y. Li, *Bioresour. Technol.*, 2020, **315**, 123788.
74 S. Bagchi and M. Behera, *Bioelectrochemistry*, 2019, **129**, 206–210.
75 S. Das, I. Chakraborty, P. P. Rajesh and M. M. Ghangrekar, *J. Hazard., Toxic Radioact. Waste*, 2020, **24**, 1–7.
76 I. Chakraborty, G. D. Bhowmick, D. Ghosh, B. K. Dubey, D. Pradhan and M. M. Ghangrekar, *Sustainable Energy Technol. Assessments*, 2020, **42**, 100808.
77 Y. Zhang, B. Min, L. Huang and I. Angelidaki, *Bioresour. Technol.*, 2011, **102**, 1166–1173.
78 N. S. Malvankar, M. T. Tuominen and D. R. Lovley, *Energy Environ. Sci.*, 2012, **5**, 5790–5797.
79 S. Prathiba, P. S. Kumar and D. V. N. Vo, *Chemosphere*, 2022, **286**, 131856.
80 S. Shapiro-Bengtsen, L. Hamelin, L. Bregnbæk, L. Zou and M. Münster, *Energy Environ. Sci.*, 2022, 1950–1966.
81 Z. Zhao, S. Qi, R. Wang, H. Li, G. Song, H. Li and Q. Yin, *Int. J. Hydrogen Energy*, 2024, **52**, 122–132.